Colloids and Surfaces A: Physicochemical and Engineering Aspects 702 (2024) 135185

Contents lists available at ScienceDirect

Colloids and Surfaces A: Physicochemical and Engineering Aspects

journal homepage: www.elsevier.com/locate/colsurfa

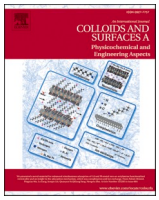

Micro container made of levitated liquid bead

Aditya Vashi *, Ajeet Singh Yadav, Nam-Trung Nguyen

Queensland Micro and Nanotechnology Centre, Griffith University, 170 Kessels Road, Nathan, Queensland 4111, Australia

GRAPHICAL ABSTRACT

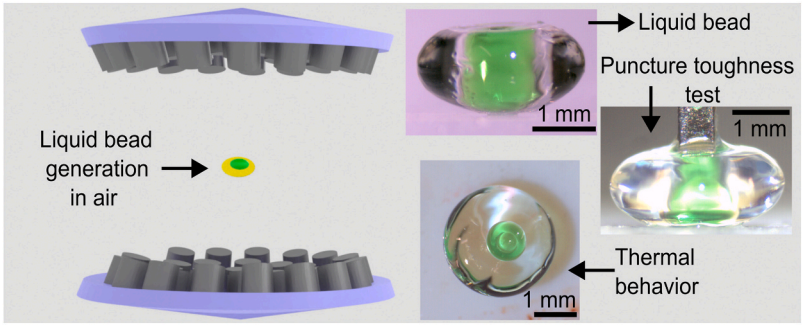

ARTICLE INFO

Keywords:
Digital microfluidics
Liquid bead
Acoustic levitation
Micro container
Puncture toughness
Thermal behaviour

ABSTRACT

Liquid bead, an emerging digital microfluidic platform offers a wide range of applications in research and industry. Making liquid beads using acoustic levitation technology allows for the fabrication of micro container. Extensive insight into levitated liquid beads is essential for determining their performance. Firstly, this paper unfolds the unique interface of the levitated liquid bead, which has thin membrane of shell material on top and thus serves as a micro container. Next, we characterised the puncture toughness of liquid beads to assess the capability of releasing the liquid content. Liquid bead with larger corresponding shell volume and lower core volume recorded the highest resistance against needle penetration. Finally, we observed the thermal behaviour of liquid beads at elevated temperature. The liquid beads showed no morphological change over 10-minutes period at 50 °C. At 65 °C, liquid bead exceeded the critical temperature threshold, which resulted in breaking the thin membrane and releasing the liquid from the core.

1. Introduction

Digital microfluidics (DMF) is an advanced technology that handles liquid in discrete droplets with size ranging from picolitre to microlitre, instead of a continuous fluid flow [1]. DMF technology has opened up new applications in chemistry, biology, and medicine due to low reagent consumption, fast reaction, negligible contamination, and easy integration with analytical tools [1]. Liquid droplet, liquid marble [2], and liquid bead [3] are three major DMF platforms to perform tasks such as dispensing, merging, splitting, mixing, and sorting. Liquid marbles are liquid droplets coated with micro- or nanoparticles forming the porous shell around the liquid core [4]. This structure protects the liquid drop against surface wetting and contamination [4]. However, liquid marble face drawbacks in mechanical robustness and uniformity in

* Corresponding author.
E-mail address: aditya.vashi@griffithuni.edu.au (A. Vashi).

https://doi.org/10.1016/j.colsurfa.2024.135185
Received 4 July 2024; Accepted 23 August 2024
Available online 26 August 2024

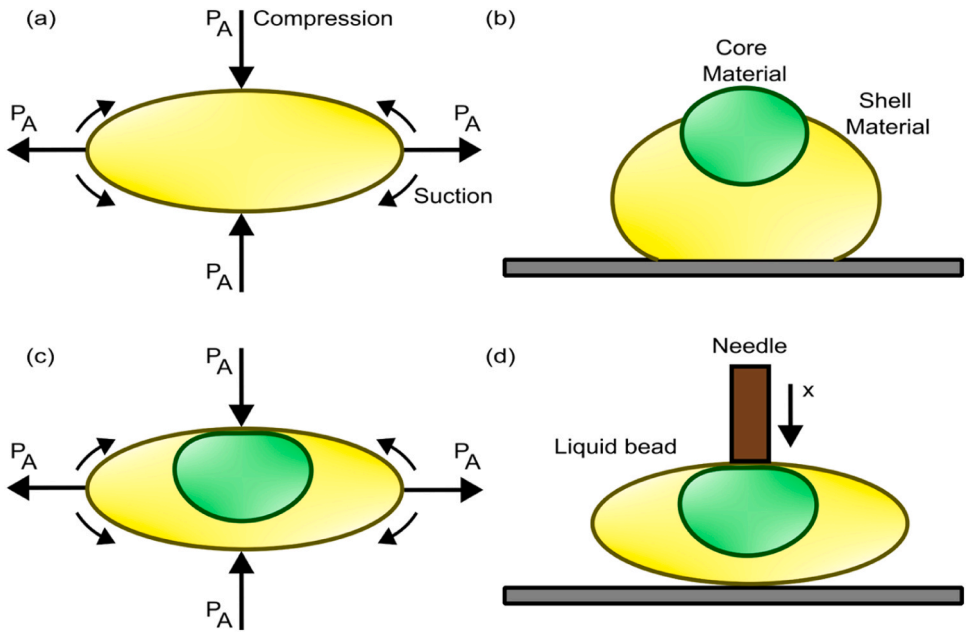

Fig. 1. (a) Acoustic radiation pressure on a levitated compressible object. Configuration of liquid core and shell material (b) without acoustic levitation and (c) in acoustic levitation. (d) Schematic model of puncture toughness test.

terms of size, shell thickness, and porosity [5].

Liquid bead is an emerging DMF platform, which have solid shell encapsulating a liquid core, providing better robustness and uniformity compared to liquid marbles [6]. Because of their solid shell, liquid beads not only prevent contamination but also offer the capability for long-term storage or controlled release of the core liquid, serving as a microcontainer. The advantages of liquid beads opened up practical real-world application, such as culturing cells [7] and microalgae [8], amplification of deoxyribonucleic acid (DNA) for polymerise chain reaction [9], food processing [10], and cosmetics [11]. Most common liquid beads generation methods include polymerisation, droplet extrusion, coaxial electrospinning, and microfluidic droplet formation [12,13]. Although the methods mentioned above have matured in generating liquid beads on earth, no efforts have been made to explore their generation in the microgravity environment of space. The major reasons to this limitation are complex setup, liquid handling, and modification of devices for space experiment.

Levitation is the technique that suspends materials in air or other medium counteracting the gravity with other forces, such as optical [14], acoustic [15], magnetic [16], aerodynamic [17], and electrostatic [18]. Comparing with other levitation techniques, acoustic levitation can hold any material using sound waves, without the need of any specific magnetic or optic property [19]. In acoustic levitation, gravitational force only changes the levitation position, and have very minor effect in the equilibrium shape of the compressible material [20]. As a result, acoustic levitation can be employed in space without the need for any modification of the levitation device. In addition, acoustic levitation devices are cost effective, less complex, and require less space. These advantages have led acoustic levitation applications in material science [21], fluid dynamics [22], analytical chemistry [23], and microgravity research [24]. Recently, acoustic levitation capability has been extended to three-dimensional (3D) cell culture [25] and fabricating complex artificial cells [26]. Tang et al. employed acoustic levitation to form liquid bead with magnetic core [27]. The team further characterised the liquid beads response in the magnetic field using microfluidic channel [27].

Generation of liquid beads with acoustic levitation provide unique opportunity for DMF on earth as well as in space. For that, understanding the properties of levitated liquid bead is crucial for their design, handling, and application. To the best of our knowledge, no previous study has explored the different properties of airborne liquid beads. In this paper, we generated liquid beads with commercially available, low-cost, and easy to build acoustic levitator. We used DI water as a core liquid and photopolymer as shell liquid to form a liquid bead. We investigated the shape of the liquid bead for different volume of core liquid and shell liquid. Liquid beads produced with acoustic levitation have distinct structure, creating the thin membrane of shell material on top, that serves as the cap of the micro container. We determined the mechanical property of liquid bead by characterising the puncture toughness for eventual release of the core liquid. Finally, we demonstrated thermal behaviour of liquid beads as micro containers at elevated temperature.

2. Theoretical background

2.1. Acoustic radiation pressure

An object experiences acoustic radiation pressure on the surface when levitated in acoustic field. For liquid droplet, acoustic radiation pressure also plays crucial role in determining its shape, Fig. 1a. The exerted acoustic radiation pressure on the surface can be calculated according to King's theory [28],

$$P_A = \frac{1}{2\rho_0 c_0^2} < p^2 > - \frac{1}{2}\rho_0 < v^2 > \quad (1)$$

where, p and v are the sound pressure and particle velocity, ρ_0 density of medium air, c_0 is the sound velocity in air. $< >$ denotes the time average over period of acoustic oscillation. The distribution of acoustic radiation pressure over the surface is not uniform. It is positive (compression) at polar area and negative (suction) at the equator, Fig. 1a [29]. This causes the droplet to adopt an ellipsoidal shape, which can be adjusted by varying the sound pressure, Fig. 1a.

2.2. Configuration of liquid bead in acoustic levitation

Without acoustic levitation, the liquid core forms a small lens shape on top of sessile shell drop as shown in Fig. 1b [30,31]. This configuration makes it challenging to achieve full encapsulation of the core

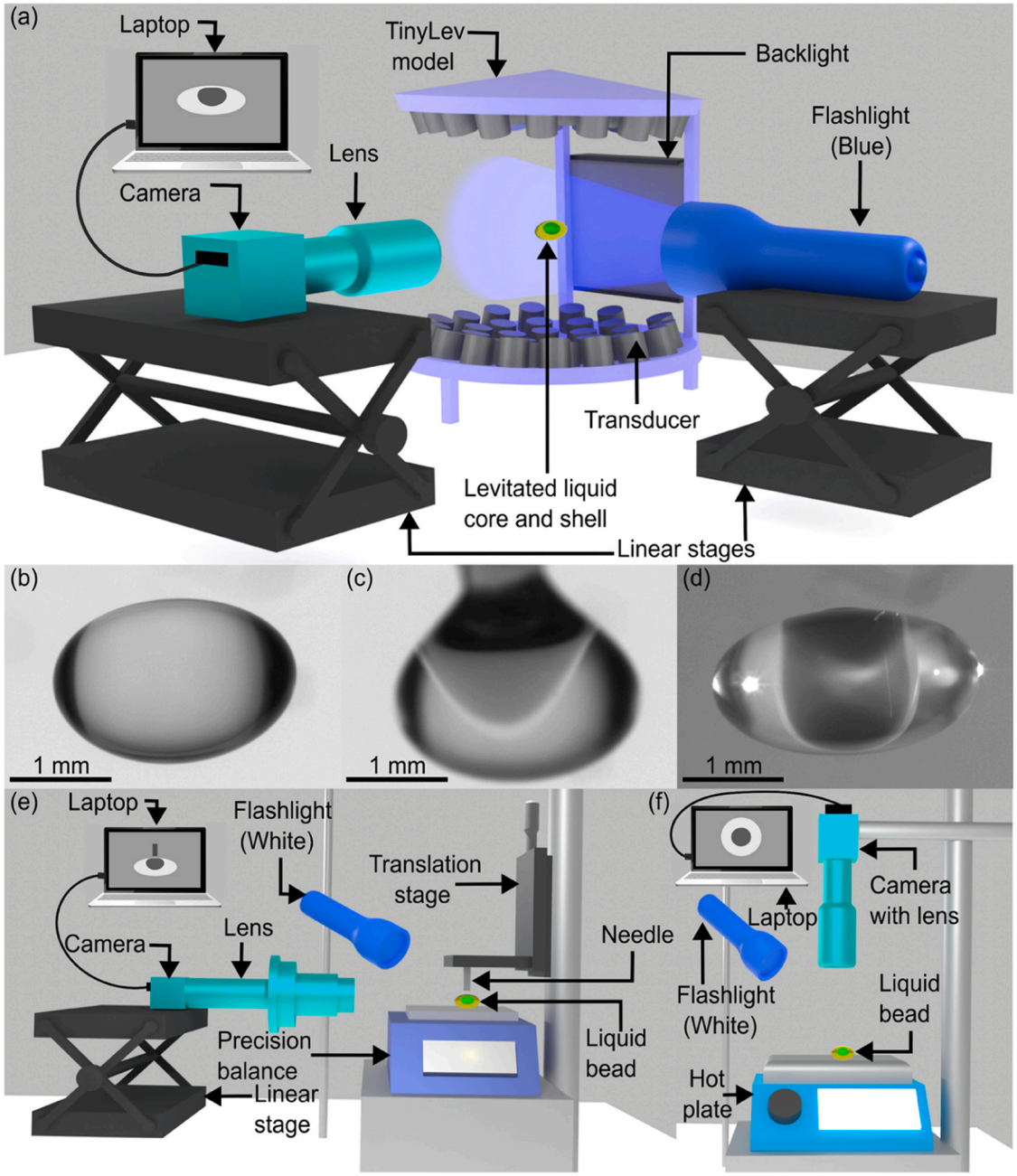

Fig. 2. (a) Experiment setup for the generation of liquid bead. (b) Levitated 5 μl shell liquid drop. (c) Insertion of 0.5 μl core liquid from top. (d) Solidification of levitated core-shell configuration in air. Schematic for the investigation of (e) puncture toughness, and (f) thermal behaviour.

within the shell liquid to generate the liquid bead. In acoustic levitation, the constant positive acoustic radiation on top surface forces the core inside shell and form the full encapsulation, Fig. 1c. Solidifying the encapsulated core inside the shell liquid with acoustic levitation can successfully generates liquid bead.

2.3. Puncture toughness of liquid beads

The liquid core remains near the top surface of the solid shell, creating a thin membrane between the core and shell of liquid bead, Fig. 1c. The membrane serves as the cap. This feature allows the liquid bead to serve as a microcontainer, which can release the core liquid if the thin cap is broken. We utilised a needle with a square tip surface to break the capping membrane to characterise the puncture toughness of liquid bead, Fig. 1d. Puncture toughness (G_P) is the total work per area needed to initiate the crack and given by [32],

$$G_P = \frac{W}{A} \tag{2}$$

where, W is the total work input and A is the surface of the affected liquid bead area which is equal to needle's tip surface area. Relation between work and force described as:

$$W = \int_{x=0}^{x=x_i} F_i(x)dx = G_p A \tag{3}$$

where, F_i is the insertion force, and x_i is the puncture position. Moreover, the insertion force is the exponential function of the insertion axis x and written as [33]:

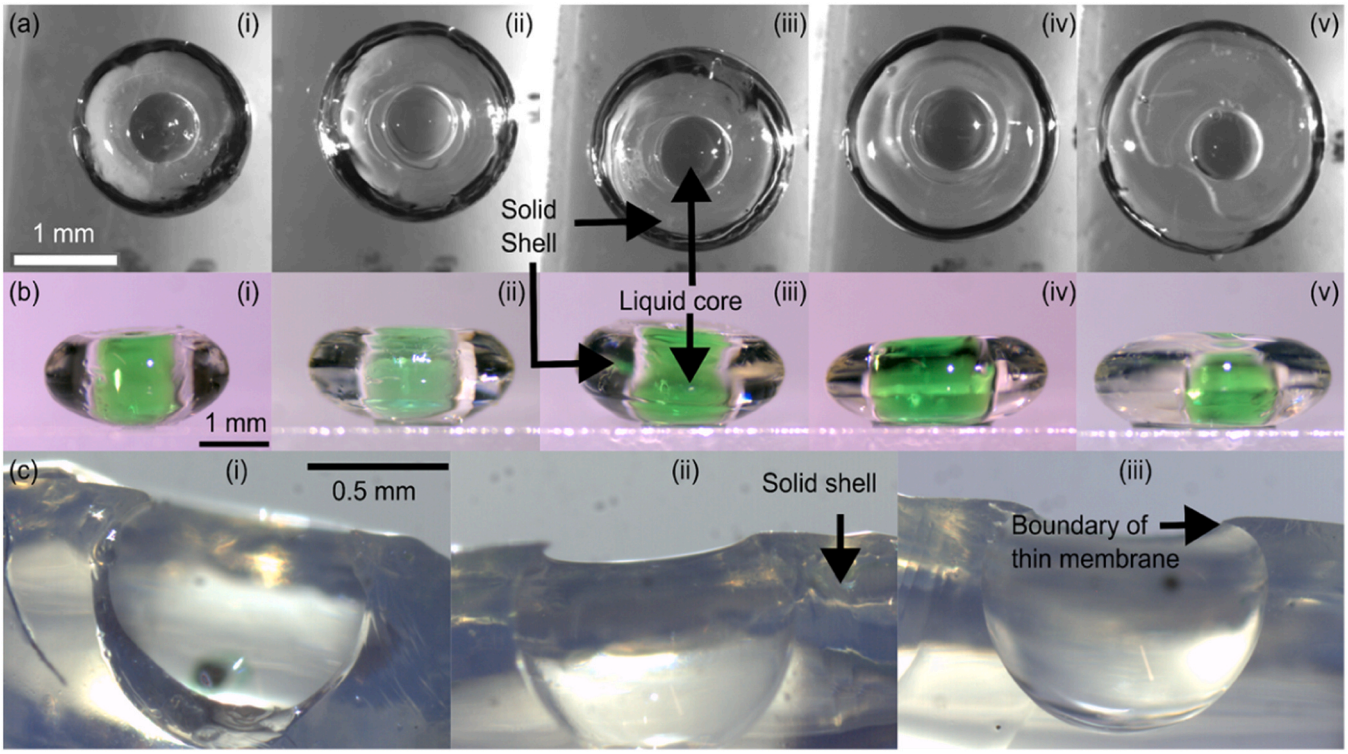

Fig. 3. (a) Top view of multiple liquid beads. (b) Side view of multiple liquid beads. (c) Cross section of liquid bead.

$$F_i(x) = F_0 \exp^{\left(\frac{x}{\chi}\right)} \tag{4}$$

where F_0 is initial insertion force, and χ is consider as characteristic length [33]. Substituting Eq. (4) in Eq. (3) results in,

$$W = F_0 \chi \exp^{\left(\frac{x_i}{\chi}\right)} - F_0 \chi = G_p A \tag{5}$$

$$F_i(\max) = F_0 + \frac{1}{\chi} G_p A \tag{6}$$

We determine the F_0, and χ through exponential curve fitting across all experiment for different liquid beads. Moreover, puncture toughness of the liquid bead can be obtained at maximum insertion force and derived as:

$$G_p = \frac{\chi}{A}(F_i(\max) - F_0) \tag{7}$$

3. Material and methods

3.1. Material preparation

The shell of the liquid bead comprised of 0.06 g ethyl- 4(dimethyl amino) benzoate (Merck), 0.05 g camphorquinone (Merck), and 10 g of trimethylolpropane trimethacrylate (TMPTMA, Merck). Shell materials were mixed using magnetic stirrer at 600 rpm for 1 hour. We mixed 0.5 ml of DI water with 0.005 ml green colour dye (Queen Fine Foods) as the core material of liquid bead.

3.2. Liquid bead generation setup and procedure

Fig. 2a illustrates the experiment setup to generate the elevated liquid beads. The acoustic levitator "TinyLev" was used for the suspension of shell and core liquids [34]. The transducers in TinyLev device operates at 40 kHz. The 40 kHz signal was excited through nanoArduino and L297N dual H-bridge stepper motor driver. The device was powered by a variable DC power supply (Keithley 2200–30–5). The droplets of shell and core liquids were dispensed with two different micropipettes, Eppendorf Research plus – 3123000039 and LLG 9280001, respectively. The blue flashlight (NiteCore CB6) was used for the solidification of shell liquid. The levitation process was observed and recorded using camera (XIMEA USB 3.0 1.3 MP B/W) connected with telecentric lens (Edmund Optics 1.0 × SilverTLTM).

Initially, 5 µl of shell liquid was suspended at the centre node of the acoustic cavity with a driving voltage of 7 V, Fig. 2b. Subsequently, 0.5 µl of core liquid was added from the top to establish the core-shell configuration, Fig. 2c. The levitated droplet was then exposed to blue light for a duration of 20 minutes to solidify the shell, Fig. 2d. Once solidified, the bead was collected in DI water. We conducted three repetitions of the experiment to ensure successful generation of liquid beads with the desired volume ratios. Apart from 0.5 µl, we encapsulated core volumes of 1 µl and 1.5 µl in 5 µl of shell liquid. However, after three trials, the encapsulation of 2 µl of core liquid in 5 µl of shell liquid was not successful. Furthermore, we conducted experiments with varying shell volumes, incrementing by 2.5 µl. We successfully levitated shell volumes of 7.5 µl and 10 µl at the node by adjusting the driving voltage between 6.7 and 7.3 V. However, consistent levitation of 12.5 µl was not achieved. At a higher voltage, the droplet bursted, while at lower voltages, it dropped in the cavity. Similar to 5 µl shell volume, core volumes of 0.5 µl, 1 µl, and 1.5 µl were encapsulated with 7.5 µl and 10 µl shell volume to form liquid beads.

3.3. Experiment setup for puncture toughness and thermal behaviour test

Fig. 2e shows the schematic for puncture toughness test. Rectangle needle (electronic pin) was fixed on the right-angle mounting adapter with a single-axis translation stage consist of standard micrometre position. A liquid bead is placed on a precision balance. The side view of the liquid bead was recorded using camera (XIMEA USB 3.0 1.3 MP RGB) connected with zoom imaging lens (Edmund Optics VZMTM 450). The needle was moved downward with increment of 0.05 mm to

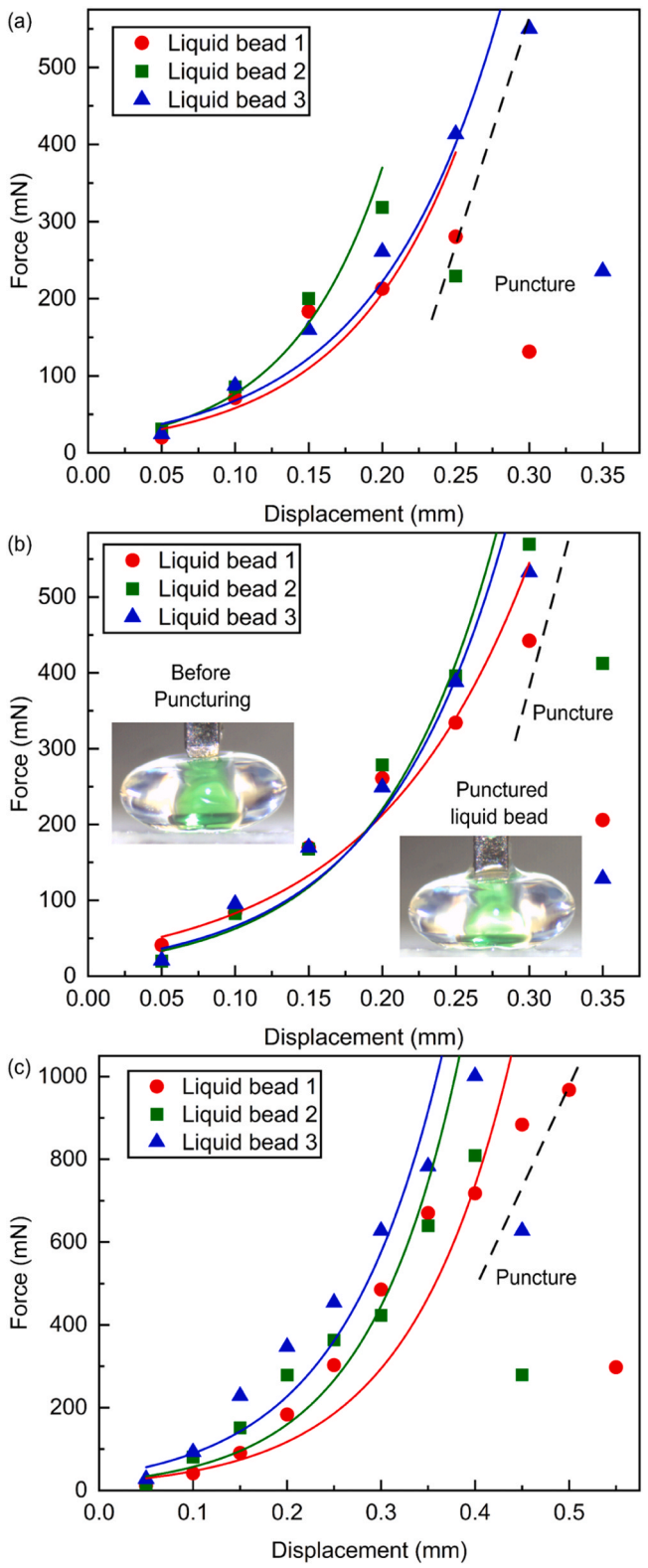

Fig. 4. Force vs. displacement characteristic of different liquid beads with core liquid 0.5 μl and corresponding shell volume (a) 5 μl, (b) 7.5 μl and (c)10 μl.

puncture the liquid bead. The applied load on liquid bead was measured with the precision balance. The force acting on the liquid bead for corresponding displacement to puncture the bead was calculated to determine the puncture toughness of the liquid bead.

Thermal behaviour of liquid beads was carried out on a controlled hot plate as shown in Fig. 2f. Elevated temperature increases the pressure inside the liquid core. At critical temperature, pressure exceeds the strength of thin membrane and ruptured it. At first, we examined the liquid beads stability at elevated temperature 50 °C for 10 minutes in ambient condition. If no change was observed, we increased the temperature by 15 °C step until the liquid bead ruptured at a critical temperature. The process was monitored from the top using a camera (XIMEA USB 3.0 1.3 MP RGB) and lens (Edmund Optics 1.0 × SilverTLTM).

4. Result and discussion

4.1. Liquid bead morphology

Fig. 3 depicts the liquid beads observed from different perspectives. Fig. 3a and b represents the top view and side view of the multiple liquid beads, repectively. Fig. 3a and b (i), (ii), and (v) depict the liquid beads with the core volume 0.5 μl and the corresponding shell volumes 5, 7.5 and 10 μl, respectively. Fig. 3a, and b (iii) and (iv) show the liquid beads with corresponding shell volume 7.5 μl and core volumes of 1 and 1.5 μl. The top view of multiple liquid beads validated the core position inside the bead near to the centre. It is important to note that, this position mainly relied on the initial insertion process. Liquid core away from the centre and near to edge did not result in successful encapsulation after solidification.

The side images revealed the ellipsoidal shape of the liquid bead, consistent with theoretical predictions. However, the convex surface of the solid shell magnified the liquid core inside the bead, making it difficult to determine the exact position of the core liquid from the side images. To investigate further, we cut the liquid bead with a scalpel and examined its cross-section. Fig. 3c shows the cross-section view of different liquid beads. The corresponding shell volumes were 5, 7.5 and 10 μl with a core volume of 0.5 μl for Fig. 3c (i), (ii), and (iii) respectively. The shape of the core was ellipsoidal inside the solid shell. However, the acoustic radiation pressure compressed the top surface, causing it to flatten. This deformation was evident in the shape of the core. The thin membrane disintegrated during the cutting process. But we could visualise the boundary of the thin membrane. This boundary verified the complete encapsulation of the liquid bead in acoustic levitation.

4.2. Puncture toughness of liquid beads

Fig. 4 illustrates the force - displacement relationship for three liquid beads with core volume 0.5 μl and c shell volumes of 5 μl (Fig. 4a), 7.5 μl (Fig. 4b) and 10 μl (Fig. 4c). However, the needle directly penetrated inside the core without showing significant change on the precision balance for core liquid with a volume of more than 0.5 μl. As shown in Fig. 4, the force started to increase as the needle displacement increases. The force decreased sharply once the needle punctured the thin membrane of shell as shown in Fig. 4. It is interesting to note that, at lower displacement the generated force was similar, which diverged at higher displacement for all the different liquid beads. The results indicate that the liquid beads exhibited increasing resistance as the compression displacement increased.

Liquid beads punctured within the 0.2–0.3 mm displacement range with the required maximum force ranging from 300 to 550 mN for the shell volume of 5 μL, Fig. 4a. For the shell volume of 7.5 μL, the needle penetrated after 0.3 mm for all three liquid beads, Fig. 4b. The maximum force varied from 400 to 600 mN, demonstrating an increase in mechanical strength compared to beads with a smaller shell volume. The displacement range increased to 0.4–0.5 mm with maximum force ranging from 800 to 1000 mN for a shell volume of 10 μL. This substantial increase in both displacement and force demonstrated the higher mechanical robustness of these beads. The results suggest increased thickness of thin membrane layer with corresponding shell

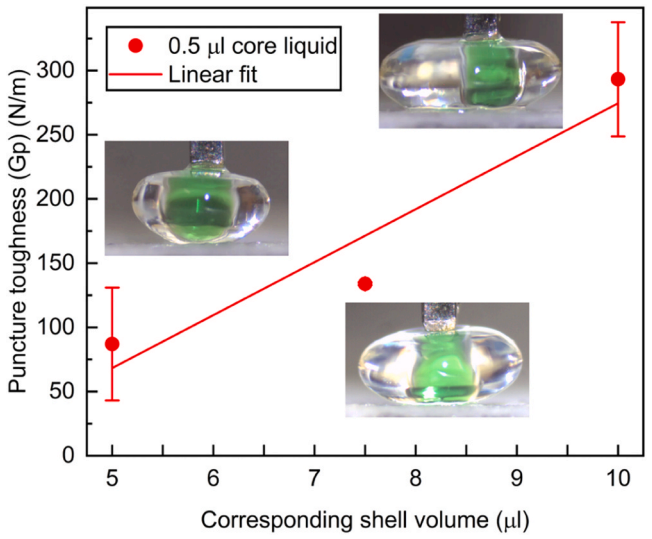

Fig. 5. Puncture toughness of liquid bead for core liquid 0.5 µL at different corresponding shell volume.

volumes. Moreover, the variation in the displacement and force for same corresponding shell and core liquid was attributed to differences in their internal structure discuss in above section.

Next, we characterised the liquid bead with puncture toughness. We fitted all the data with exponential curve and obtained initial insertion force and characteristic length for each bead as per the theory. The needle bottom surface area was 0.325 mm^2. From the acquired values, we measured the puncture toughness for each bead using Eq. (7). Fig. 5 depicts the relationship of puncture toughness with corresponding shell volume of liquid beads for 0.5 µl. The average puncture toughness for 5 µl shell volume was 87 N/m and increased to 137 N/m for 7.5-µl shell volume. The liquid bead with corresponding shell volume of 10 µl had the highest average puncture toughness of 293 N/m.

4.3. Thermal behaviour of liquid beads

We further investigated the thermal stability of liquid beads with a core volume of 0.5 µl over a 10-minute period as these liquid beads had shown higher robustness compared to others. The experiment was carried out for three different samples. Fig. 6a (i), (ii) and (iii) show the thermal behaviour of liquid beads at 50 °C for shell volumes of 5, 7.5 and 10 µl, respectively. No morphological changes were observed in the liquid beads over a 10-minute period, indicating good stability at 50°C.

Next, we investigated the liquid beads at 65 °C. Fig. 6b (i), (ii) and (iii) show the liquid beads morphology at 65 °C for corresponding shell volumes of 5, 7.5 and 10 µl, respectively. All liquid beads ruptured within 10 minutes. We could observe the ruptured thin membrane at 10 minutes. This result showed that 65 °C exceeded the critical temperature threshold for all liquid beads. Ruptured thin membrane resulted in releasing the liquid core from the liquid beads serving as micro containers.

5. Conclusion

In this paper, we generated micro containers in the form of liquid beads with acoustic levitation for different shell volume and core volumes. Ellipsoidal shape and convex surface of liquid bead magnified the liquid core, preventing the exact characterisation of the shape and position of the core. The cross-section analysis of liquid beads confirmed

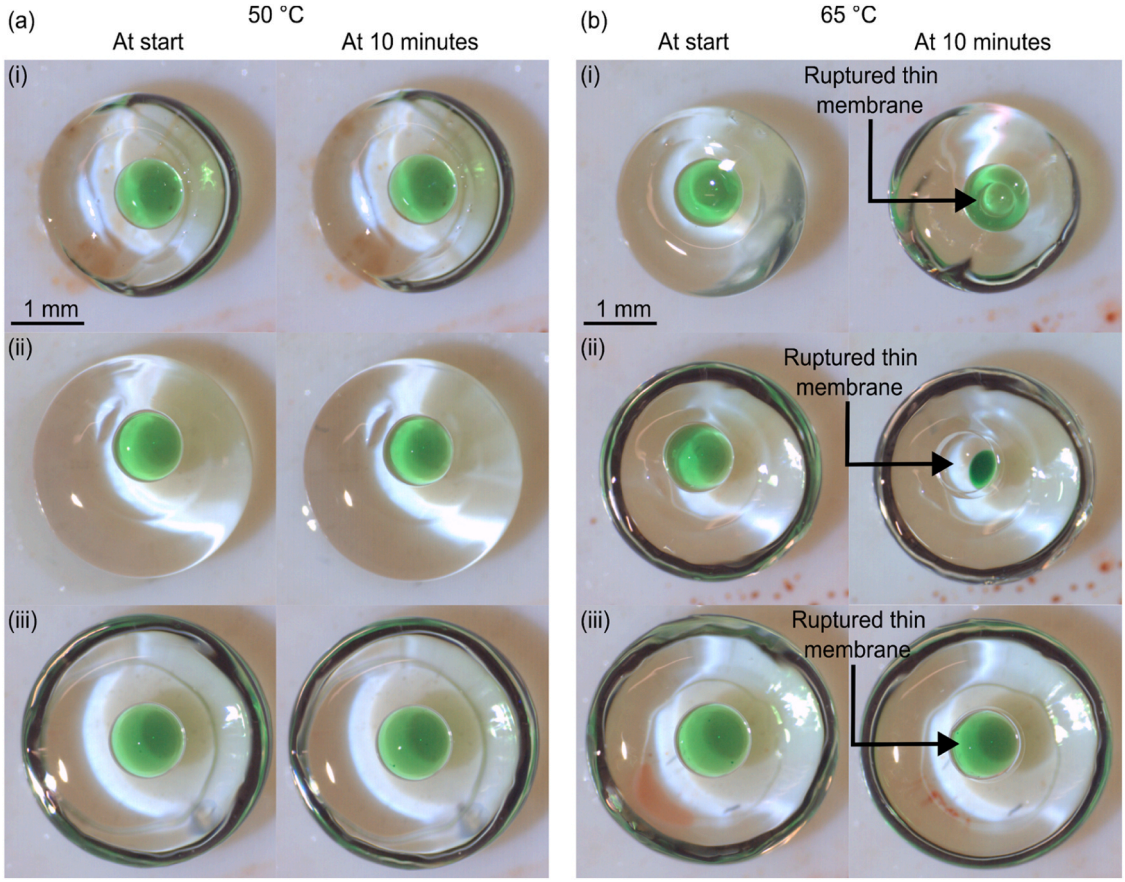

Fig. 6. Thermal behaviour of different liquid beads (a) at 50 °C and (b) 65 °C.

the core liquid position near top of the shell creating a thin membrane, acting as the cap of the micro container. We evaluated the thin membrane of liquid bead with puncture toughness. Liquid core with 0.5 μl have more robustness compared to liquid core with 1 and 1.5 μl. We revealed increasing puncture toughness of liquid bead with increasing shell volume for same core liquid indicating increased membrane thickness of liquid bead. Further, we investigated the thermal behaviour of more robust liquid beads. Liquid beads were thermally stable up to 50 °C. At 65 °C liquid beads surpassed the critical temperature limit resulting in disintegration of thin membrane. Liquid bead fabricated using acoustic levitation promises potential application in liquid storage, controlled release as well as micro reaction.

Authors contribution

NTN and AV conceptualized and designed the experiments. AV and ASY performed the experiments. AV analysed the data and prepared the original manuscript and figures.

CRediT authorship contribution statement

Ajeet Singh Yadav: Formal analysis, Writing – review & editing, Investigation. **Nam-Trung Nguyen:** Conceptualization, Methodology, Supervision, Writing – review & editing. **Aditya Vashi:** Conceptualization, Data curation, Formal analysis, Writing – original draft, Methodology, Investigation, Validation.

Declaration of Competing Interest

The authors declare that they have no known competing financial interests or personal relationships that could have appeared to influence the work reported in this paper

Data availability

Data will be made available on request.

Acknowledgements

We are grateful to griffith university for provinding faclities to carry out the research. We thanks the funding support from the Griffith University International Postgraduate Research Scholarship. NTN acknowleges funding support from the Australian Research Council, project DP220100261.

References

[1] K. Choi, et al., Digital microfluidics, Annu. Rev. Anal. Chem. 5 (1) (2012) 413–440.
[2] P. Aussillous, D. Quéré, Liquid marbles, Nature 411 (6840) (2001) 924–927.
[3] A.S. Yadav, et al., Synthesis and active manipulation of magnetic liquid beads, Biomed. Micro 26 (2) (2024) 24.
[4] C.H. Ooi, N.-T. Nguyen, Manipulation of liquid marbles, Microfluid. Nanofluidics 19 (2015) 483–495.
[5] C.H. Ooi, et al., Liquid marble-based digital microfluidics–fundamentals and applications, Lab a Chip 21 (7) (2021) 1199–1216.
[6] D.T. Tran, et al., Biodegradable polymers for micro elastofluidics, Small (2023) 2303435.
[7] Q. Sun, et al., Microfluidic formation of coculture tumor spheroids with stromal cells as a novel 3D tumor model for drug testing, ACS Biomater. Sci. Eng. 4 (12) (2018) 4425–4433.
[8] D.T. Tran, et al., Calcium alginate elastic capsules for microalgal cultivation, RSC Adv. 14 (22) (2024) 15441–15448.
[9] A.S. Yadav, et al., Precise, wide field, and low-cost imaging and analysis of core–shell beads for digital polymerase chain reaction, Lab a Chip 23 (15) (2023) 3353–3360.
[10] Q. Wu, et al., Preparation of alginate core–shell beads with different M/G ratios to improve the stability of fish oil, LWT 80 (2017) 304–310.
[11] A.F. Bonda, et al., Alginate/maltodextrin and alginate/shellac gum core-shell capsules for the encapsulation of peppermint essential oil, Int. J. Biol. Macromol. 162 (2020) 1293–1302.
[12] H.N. Yow, A.F. Routh, Formation of liquid core–polymer shell microcapsules, Soft Matter 2 (11) (2006) 940–949.
[13] R.A. Ramli, W.A. Laftah, S. Hashim, Core–shell polymers: a review, RSC Adv. 3 (36) (2013) 15543–15565.
[14] A. Ashkin, J. Dziedzic, Optical levitation by radiation pressure, Appl. Phys. Lett. 19 (8) (1971) 283–285.
[15] E.H. Brandt, Suspended by sound, Nature 413 (6855) (2001) 474–475.
[16] Jayawant, B.V., Electromagnetic levitation and suspension techniques. 1981.
[17] L. Hennet, et al., Aerodynamic levitation and laser heating, Eur. Phys. J. Spec. Top. 196 (1) (2011) 151–165.
[18] W.-K. Rhim, et al., Noncontact technique for measuring surface tension and viscosity of molten materials using high temperature electrostatic levitation, Rev. Sci. Instrum. 70 (6) (1999) 2796–2801.
[19] M.A.B. Andrade, N. Pérez, J.C. Adamowski, Review of progress in acoustic levitation, Braz. J. Phys. 48 (2) (2018) 190–213.
[20] W. Xie, B. Wei, Dynamics of acoustically levitated disk samples, Phys. Rev. E 70 (4) (2004) 046611.
[21] D. Geng, et al., Extraordinary solidification mechanism of liquid alloys under acoustic levitation state, Adv. Mater. (2022) 2206464.
[22] A. Vashi, et al., The dynamics of vertical coalescence of acoustically levitated droplets, Microfluid. Nanofluidics 28 (5) (2024) 34.
[23] S. Santesson, S. Nilsson, Airborne chemistry: acoustic levitation in chemical analysis, Anal. Bioanal. Chem. 378 (7) (2004) 1704–1709.
[24] A. Vashi, et al., Parametric analysis of acoustically levitated droplet for potential microgravity application, Appl. Acoust. 213 (2023) 109624.
[25] N. Jeger-Madiot, et al., Self-organization and culture of mesenchymal stem cell spheroids in acoustic levitation, Sci. Rep. 11 (1) (2021) 8355.
[26] J. Li, et al., Building programmable multicompartment artificial cells incorporating remotely activated protein channels using microfluidics and acoustic levitation, Nat. Commun. 13 (1) (2022) 4125.
[27] T. Tang, et al., Acoustic levitation-assisted contactless printing of microdroplets for biomedical applications, J. Manuf. Sci. Eng. 146 (1) (2024) 011002.
[28] L.V. King, On the acoustic radiation pressure on spheres, Proc. R. Soc. Lond. Ser. A Math. Phys. Sci. 147 (861) (1934) 212–240.
[29] D. Zang, et al., Inducing drop to bubble transformation via resonance in ultrasound, Nat. Commun. 9 (1) (2018) 3546.
[30] M.J. Neeson, et al., Compound sessile drops, Soft Matter 8 (43) (2012) 11042–11050.
[31] K.R. Sreejith, et al., Core-shell beads made by composite liquid marble technology as a versatile microreactor for polymerase chain reaction, Micromachines 11 (3) (2020) 242.
[32] S.P. Davis, et al., Insertion of microneedles into skin: measurement and prediction of insertion force and needle fracture force, J. Biomech. 37 (8) (2004) 1155–1163.
[33] N.-T. Nguyen, S.T. Wereley, S.A.M. Shaegh, Fundamentals and Applications of Microfluidics, Artech house, 2019.
[34] A. Marzo, A. Barnes, B.W. Drinkwater, TinyLev: a multi-emitter single-axis acoustic levitator, Rev. Sci. Instrum. 88 (8) (2017) 085105.